Vol. 55, No. 4

In Vitro Characterization of GS-8374, a Novel Phosphonate-Containing Inhibitor of HIV-1 Protease with a Favorable Resistance Profile[▽][†]

Christian Callebaut,[1]* Kirsten Stray,[1] Luong Tsai,[1] Matt Williams,[1] Zheng-Yu Yang,[1]
Carina Cannizzaro,[1] Stephanie A. Leavitt,[1] Xiaohong Liu,[1] Kelly Wang,[1]
Bernard P. Murray,[1] Andrew Mulato,[1] Marcos Hatada,[1] Tina Priskich,[2]
Neil Parkin,[2]‡ Swami Swaminathan,[1] William Lee,[1] Gong-Xin He,[1]
Lianhong Xu,[1] and Tomas Cihlar[1]

Gilead Sciences, Inc., Foster City, California,[1] and Monogram Biosciences, South San Francisco, California[2]

GS-8374 is a novel bis-tetrahydrofuran HIV-1 protease (PR) inhibitor (PI) with a unique diethylphosphonate moiety. It was selected from a series of analogs containing various di(alkyl)phosphonate substitutions connected via a linker to the *para* position of a P-1 phenyl ring. GS-8374 inhibits HIV-1 PR with high potency ($K_i = 8.1$ pM) and with no known effect on host proteases. Kinetic and thermodynamic analysis of GS-8374 binding to PR demonstrated an extremely slow off rate for the inhibitor and favorable contributions of both the enthalpic and entropic components to the total free binding energy. GS-8374 showed potent antiretroviral activity in T-cell lines, primary CD4$^+$ T cells (50% effective concentration [EC_{50}] = 3.4 to 11.5 nM), and macrophages (EC_{50} = 25.5 nM) and exhibited low cytotoxicity in multiple human cell types. The antiviral potency of GS-8374 was only moderately affected by human serum protein binding, and its combination with multiple approved antiretrovirals showed synergistic effects. When it was tested in a PhenoSense assay against a panel of 24 patient-derived viruses with high-level PI resistance, GS-8374 showed lower mean EC_{50}s and lower fold resistance than any of the clinically approved PIs. Similar to other PIs, *in vitro* hepatic microsomal metabolism of GS-8374 was efficiently blocked by ritonavir, suggesting a potential for effective pharmacokinetic boosting *in vivo*. In summary, results from this broad *in vitro* pharmacological profiling indicate that GS-8374 is a promising candidate to be further assessed as a new antiretroviral agent with potential for clinical efficacy in both treatment-naïve and -experienced patients.

Fifteen years ago, HIV protease (PR) inhibitors (PIs) were introduced into the clinic as a second class of antiretrovirals, after nucleosides, and launched the era of combination antiretroviral therapy (ART) that brought along a dramatic reduction of the morbidity and mortality among HIV-infected patients (7, 25, 29, 46). PIs evolved to be an important class of agents that are being widely used in combination with other antiretrovirals in both treatment-naïve and -experienced patients (48). On the basis of recent revisions of HIV treatment guidelines, one of several ritonavir-boosted PIs is recommended for use as a third agent of choice in combination with tenofovir and emtricitabine for first-line ART (8, 53). The choice of PIs over other antiretroviral agents is primarily driven by their clinical potency and a higher genetic barrier for resistance development (48). In addition, the clinical use of more recently developed PIs with improved resistance profiles, e.g., darunavir, in combination with new antiretrovirals may represent a promising nucleoside-sparing option for highly treatment-experienced patients (13, 50).

Although a total of nine PIs is currently available for the treatment of HIV infection, only a few are widely used. In general, the long-term clinical benefit of PIs across all patient populations can be limited by various factors, including long-term safety and tolerability (3, 27, 38), resistance (36), and drug-drug interactions (18). Among these limitations, the development of viral resistance has been shown to be a major cause of therapy failure (1, 43). Several studies revealed that a significant proportion of patients with detectable viral loads harbor HIV strains resistant to at least one PI (36, 44). Furthermore, transmission of resistant viruses, including strains with reduced susceptibility to approved PIs, has been documented and may limit the choices for the first-line therapy (17, 47). The structural similarity among the multiple PIs used in the clinic increases the possibility of cross-resistance within this therapeutic class (52). Consequently, the mutations conferring resistance are frequently common to multiple PIs (14, 45). Therefore, the design of novel PIs with more favorable resistance profiles and improved pharmacological properties remains an area of high interest.

Over more than 2 decades of intense development, HIV therapy became a complex and quickly evolving field of medical research. Novel therapeutic concepts and regimens using both the established and new antiretroviral drug classes are being explored with a primary goal to address limitations of ART in various patient populations. Increasing age of HIV-infected patients brings about additional challenges, such as long-term effects of HIV infection and tolerability of ART (15). In addition, ongoing health care reforms generate pressure to reduce treatment costs, providing an incentive for ex-

---

* Corresponding author. Mailing address: Gilead Sciences, 333 Lakeside Dr., Foster City, CA 94404. Phone: (650) 522-6362. Fax: (650) 522-5143. E-mail: christian.callebaut@gilead.com.
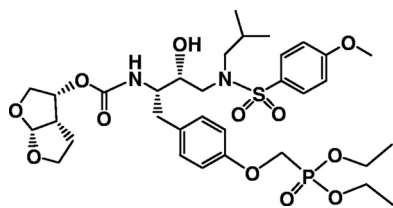‡ Present address: Data First Consulting, Menlo Park, CA.

FIG. 1. Structure of GS-8374.

ploring novel simplified treatment regimens. These evolving aspects of anti-HIV therapy create additional need for potent, durable, and well-tolerated antiretrovirals, including novel PIs.

Being aware of both the unique qualities and limitations of PIs, we explored the design of novel compounds through the application of novel modifications to established PI chemotypes. Recently, we reported on inhibitors containing a phosphonate moiety and showed that in comparison with the parent scaffolds, the phosphonate-modified compounds exhibit improved activity against a limited panel of PI-resistant viruses (4). Based on these initial data, we further explored a range of di(alkyl)phosphonate substituents in the structural context of TMC-126, a previously described bis-tetrahydrofuran (bis-THF) peptidomimetic PI (9, 10). Here and in a parallel report (12) we describe the profiling of GS-8374 (Fig. 1), a novel diethylphosphonate derivative of TMC-126 that exhibits favorable pharmacological properties, including a resistance profile superior to the profiles of all clinically approved PIs.

MATERIALS AND METHODS

Compounds. GS-8374, ($3R$,$3aS$,$6aR$)-hexahydrofuro[2,3-b]furan-3-yl ($2S$,$3R$)-1-(4-((diethoxyphosphoryl)methoxy)phenyl)-3-hydroxy-4-(N-isobutyl-4-methoxyphenylsulfonamido)butan-2-ylcarbamate, other phosphonate-containing PIs, and the control PIs (darunavir, saquinavir, ritonavir, nelfinavir, lopinavir, indinavir, amprenavir, and brecanavir) were synthesized at Gilead Sciences. Atazanavir was isolated by reverse-phase high-performance liquid chromatography (HPLC) from its therapeutic formulation (Reyataz).

Expression, purification, and X-ray crystallography of HIV-1 protease. The synthetic codon-optimized DNA encoding wild-type HIV-1 protease from strain III$_B$ was cloned in plasmid pET3b (Novagen EMD Biosciences, San Diego, CA) and expressed in *Escherichia coli* BL21(DE3) bacteria (Invitrogen, Carlsbad, CA). The culture was grown at 37°C, and protein expression was induced by the addition of isopropyl-β-D-thiogalactoside. Cells were harvested at 3 h postinduction, and the expressed enzyme was isolated and refolded as previously described (4). Conditions for the crystallization of HIV-1 protease with GS-8374 and TMC-126 and the X-ray data collection have also been described (4).

HIV protease binding assays. (i) SPR. Surface plasmon resonance (SPR) experiments were performed using a GE T100 system with HIV-1 protease immobilized on a CM5 sensor chip using standard amine coupling and then cross-linked with an additional 3-min activation using *N*-hydroxysuccinimide/1-ethyl-3-(3-dimethylaminopropyl)carbodiimide hydrochloride (20). HIV-1 PR surface densities ranged from 1,000 to 3,000 resonance units (RU) on flow cells 1, 2, and 4; flow cell 3 was mock coupled and served as a reference for data analysis. Experiments were performed in 10 mM HEPES, pH 7.4, 150 mM NaCl, 0.005% (wt/vol) surfactant P20, 3% (vol/vol) dimethyl sulfoxide (DMSO) at a temperature of 25°C. Surfaces were regenerated with a 15-s pulse of 100% ethylene glycol. Data processing included double referencing, and kinetic parameters were extracted using a global fit of a 1:1 binding model performed with Scrubber software (Biologic Software Pty. Ltd., Canberra, Australia).

(ii) ITC. Microcalorimetry experiments were performed using a VP-isothermal titration calorimetry (ITC) system (MicroCal, Inc., Northampton, MA). HIV-1 protease was prepared by dialysis in the experimental buffer (10 mM sodium acetate, pH 5.5) and diluted to 10 to 30 μM concentrations. Compound stock solutions were prepared by dissolving the weighed powders in DMSO and then making the appropriate dilution (100 to 300 μM) in the experimental buffer, with the final concentration of DMSO being 2% (vol/vol). For displacement

titration experiments, acetyl-pepstatin was added to the cell solution to yield a final concentration of 300 μM (45). Experiments were performed at 25°C. The measured binding K_a and the change in enthalpy (ΔH) were obtained by curve fitting using the competitive binding model performed with the software Origin (version 7.0; MicroCal Inc.). The change in Gibbs free energy (ΔG) and $-T\Delta S$ (where T is temperature and ΔS is the change in entropy) were calculated using the measured K_a and ΔH values (39).

Enzyme inhibition assays. (i) HIV-1 protease. The HIV-1 protease enzymatic assay was carried out in 96-well format using a fluorogenic synthetic hexapeptide substrate, (2-aminobenzoyl)Thr-Ile-Nle-(*p*-nitro)Phe-Gln-Arg (Bachem, Torrance, CA). The exact concentration of active protease was defined by active-site titration. For inhibition constant (K_i) determination, serial dilutions of the tested inhibitors were prepared in reaction buffer (100 mM ammonium acetate, pH 5.3, 1 M NaCl, 1 mM EDTA, 1 mM dithiothreitol, 10% [vol/vol] DMSO). Mixtures of the inhibitor and ~1 nM enzyme were preincubated for 15 min at 37°C. The reaction was initiated by adding substrate to a final concentration of 40 μM. Real-time reaction kinetics were measured at 37°C using a Gemini 96-well plate fluorimeter (Molecular Devices, Sunnyvale, CA) at a λ excitation of 330 nm and a λ emission of 420 nm. Apparent inhibition constant ($K_{i\text{app}}$) values were calculated using Prism, version 4 (Prism 4), software (GraphPad Software, La Jolla, CA), according to an algorithm for tight-binding competitive inhibition. K_is were calculated using the equation $K_{i\text{app}} = K_i (1 + [S]/K_m)$, where S is the substrate and the K_m value is 8 μM.

(ii) Cathepsin D. Enzyme assay with cathepsin D (Calbiochem) was carried out in 96-well format using a fluorogenic synthetic nonapeptide substrate, MOCAc-GKPILFFRLK(Dnp)DR-NH$_2$ (where Ac is acetyl and Dnp is 2,4-dinitrophenol) in 50 mM sodium acetate, pH 4.0. Mixtures of the inhibitors (including pepstatin A as a control) and enzyme were preincubated for 15 min at 37°C. The reaction was initiated by adding substrate to a final concentration of 6 μM. Real-time reaction kinetics were measured at 37°C using a Gemini 96-well plate fluorimeter at a λ excitation of 320 nm and a λ emission of 405 nm. The 50% inhibitory concentrations (IC$_{50}$s) were calculated using Prism 4 software.

(iii) 20S Proteasome. The 20S proteasome (QuantiZyme; BIOMOL International, Plymouth Meeting, PA) enzymatic assays were carried out in 96-well format as previously described (30) by using a fluorogenic peptide substrate, Suc-LLVY-AMC (where Suc is succinyl; BIOMOL International, Plymouth Meeting, PA), in a reaction buffer containing 50 mM Tris-HCl, pH 7.5, 25 mM KCl, 10 mM NaCl, 1 mM MgCl$_2$, and 0.03% (wt/vol) SDS. Inhibitors were preincubated in the reaction buffer with 375 μM substrate for 10 min at room temperature. Lactacystin and epoxymicin (Sigma, St. Louis, MO) were used as positive-control inhibitors. The reaction was initiated by adding 10 ng/μl of enzyme. Real-time reaction kinetics were measured at 37°C using a Gemini 96-well plate fluorimeter at a λ excitation of 335 nm and a λ emission of 485 nm. IC$_{50}$s were calculated using Prism 4 software.

Antiviral activity assays. (i) MT-2 and MT-4 cells. MT-2 cells (Stanford University, Palo Alto, CA) and MT-4 cells (AIDS Research and Reference Reagent Program) were maintained in RPMI 1640 medium supplemented with antibiotics and 10% (vol/vol) fetal bovine serum (FBS). Cells were passaged twice a week and kept at a density of 0.6×10^6 cells/ml. Cells were infected in bulk with HIV-1 III$_B$ (Advanced Biotechnologies Inc., Columbia, MD) at a multiplicity of infection (MOI) of 0.01 for 2 h at 37°C and mixed in 96-well plates with 5-fold serial dilutions of the tested compounds at a density of 20,000 cells/well in a final assay volume of 200 μl. Following a 5-day incubation at 37°C, the virus-induced cytopathic effect was determined using a cell viability assay. One hundred microliters medium was removed from each well and replaced with 100 μl of phosphate-buffered saline containing 1 mg/ml XTT [2,3,-bis(methoxy-4-nitro-5-sulfophenyl)-2*H*-tetrazolium-5-carboxanilide; Sigma, St. Louis, MO] and 5 μg/ml PMS (phenazine methosulfate; Sigma). Following a 1-hour incubation at 37°C, 20 μl of 2% (vol/vol) Triton X-100 was added to each well, and the absorbance was read at 450 nm with background subtraction at 650 nm. Results were processed by regression analysis (using Prism 4 software; GraphPad Software) to determine the 50% effective concentrations (EC$_{50}$s) for the tested compounds. Similar assays were performed in the presence of pooled human serum (HS; HyClone, Logan, UT), human serum albumin (HSA; Sigma), and α1-acid glycoprotein (AGP; Sigma); extrapolated EC$_{50}$s of the tested compounds in the presence of 100% serum were generated by exponential regression analysis using Prism 4 software.

(ii) CD4$^+$ T lymphocytes. Human peripheral blood mononuclear cells (PBMCs) were isolated from donor buffy coats (Stanford Blood Bank, Palo Alto, CA) using gradient centrifugation in Ficoll Paque Plus (Amersham Biosciences, Piscataway, NJ). Cells were activated for 4 to 5 days in RPMI 1640 medium with 15% (vol/vol) FBS, antibiotics, interleukin-2 (20 units/ml), and phytohemagglutinin (PHA-P; 1 μg/ml; Sigma). Human CD4$^+$ T lymphocytes were purified from

activated PBMCs by negative magnetic bead sorting on an AutoMACS apparatus using CD4$^+$ T-cell isolation kit II (Miltenyi Biotec, Auburn, CA). Cells were maintained at 1×10^6 cells/ml in RPMI 1640 medium supplemented with antibiotics and 15% (vol/vol) FBS. For single-cycle infection assay, CD4$^+$ T cells were infected with the HIV-1 BaL isolate (Advanced Biotechnologies Inc.) at an MOI of 1. After a 2-hour contact with virus at 37°C, cells were washed twice with cell culture medium containing 50% (vol/vol) FBS and were seeded into 96-well plates at 100,000 cells/well in 100 μl. Fivefold serial dilutions of the tested compounds were mixed with infected cells in a total volume of 200 μl. Thirty-six hours after the infection, cell supernatants were collected and the virus production in each sample was determined by HIV-1 p24 antigen enzyme-linked immunosorbent assay (Beckman Coulter, Miami, FL). The data were plotted as p24 production versus drug concentration, and the results were processed by regression analysis using Prism 4 software to determine EC$_{50}$s.

Cytotoxicity assays. (i) MT-2 and MT-4 cells. Cells were mixed in 96-well plates with 5-fold serial dilutions of the tested compounds at a density of 20,000 cells/well in a final assay volume of 200 μl. After a 5-day incubation at 37°C, cells were stained with XTT as described above. The cell viability was expressed as a percentage of the signal from untreated samples (0% cytotoxicity) after subtraction of the signal from samples treated with 1 μM podophyllotoxin (Sigma) (100% cytotoxicity). The concentration of each drug that reduced the cell viability by 50% (CC$_{50}$) was determined by nonlinear regression analysis using Prism 4 software.

(ii) HepG2 and HEK293T cells. HepG2 human hepatoma cells and HEK293T human kidney carcinoma cells (ATCC, Manassas, VA) were maintained in Dulbecco modified Eagle medium supplemented with 2 mM L-glutamine, 10% (vol/vol) FBS, 1 mM sodium pyruvate, and antibiotics. Cells were plated in 96-well plates at a density of 8,000 cells/well in a medium volume of 200 μl. On the next day, 100 μl of medium was removed from each sample well and replaced with fresh medium containing 5-fold serial dilutions of the tested compounds. After incubation at 37°C for 72 h, cells were stained with XTT and the data were processed as described above.

Drug combination assays. The activity of GS-8374 in combination with various antiretrovirals was determined in MT-2 cells infected with HIV-1 III$_B$. The infection was carried out as described above. Specific two-drug combinations were prepared in a 96-well plate format with 2-fold serial dilutions of drug 1 (blank and 7 concentrations) combined with 2-fold serial dilutions of drug 2 (blank and 5 concentrations) in a total volume of 50 μl/well. The tested concentrations for each drug were adjusted such that the concentration corresponding to the EC$_{50}$ was in the middle of the dilution range. Following infection with HIV-1 III$_B$, 15,000 MT-2 cells/well in a volume of 50 μl were added to plates containing prediluted combinations of the tested drugs. Controls containing infected untreated cells and infected cells treated with 300 μM tenofovir, representing 0% and 100% inhibition controls, respectively, were included on each assay plate. Each combination of two drugs was tested in three identical plates in parallel. After a 5-day incubation at 37°C, the virus-induced cytopathic effect was determined using a cell viability assay with CellTiter Glo reagent (Promega, Madison, WI). The reagent (100 μl) was added to each well, and the signal was quantified on a Victor V3 reader (Perkin Elmer, Wellesley, MA) following a 15-min incubation. The combination effect (synergy, additivity, or antagonism) of each tested pair of inhibitors was determined using MacSynergy II software (33) and a previously described algorithm (34, 35) The algorithm defines the combination effect according to a specific numeric value of a combination volume (nM$^2 \cdot$ %) calculated from the antiviral inhibition data. To determine the nature and the degree of the analyzed interactions, combination volume values were calculated at the 95% confidence level and ranked as followed: ≥100 (highly synergistic), ≥50 to <100 (slightly synergistic), ≥−50 to <50 (additive), ≥−100 to <−50 (slightly antagonistic), and <−100 (highly antagonistic).

Resistance profiling. The *in vitro* antiviral resistance profiling was performed by Monogram Biosciences (South San Francisco, CA) using the PhenoSense assay (32). GS-8374 and nine clinically approved PIs were tested against 24 recombinant HIV-1 variants containing protease and reverse transcriptase sequences derived from patients with high-level resistance to multiple PIs. The activity of each PI against the tested viruses was expressed as an absolute EC$_{50}$ and the fold change in the EC$_{50}$ relative to that for the wild-type reference strain.

In vitro metabolic stability. The *in vitro* metabolic stability of each PI and potential for pharmacokinetic enhancement were evaluated in human hepatic microsomal fractions by the *in vitro* half-life method essentially as previously described (28). Briefly, ritonavir (0 or 1 μM) was preincubated with 0.5 mg/ml pooled human hepatic microsomal fraction (BD Biosciences, Woburn, MA) in 0.05 M potassium phosphate buffer, pH 7.4, and 1 mM NADPH for 15 min at 37°C. Each PI was then added to a final concentration of 3 μM. The concentrations of each PI were then determined over 30-min incubation period by specific

liquid chromatography-tandem mass spectrometry assays, and the rates of loss corresponding to the intrinsic clearance (μl/min/mg of microsomal protein) were determined by log-linear regression. Analysis was performed using a Waters Micromass Quattro Premier XL tandem triple quadrupole mass spectrometer linked to an Agilent 1200 series HPLC system through a pneumatically assisted electrospray interface operating in positive ionization mode. Injections were made with a Leap Technologies HTC PAL autosampler, and chromatography was performed on a Phenomenex MercuryMS, Synergi 2μ Max-RP column. The initial mobile phase was 1% (vol/vol) aqueous acetonitrile containing 0.2% (vol/vol) formic acid, and the elution was achieved by use of a suitable linear gradient with increasing proportions of acetonitrile. Quantification was performed by use of the analyte-to-internal standard peak area ratio.
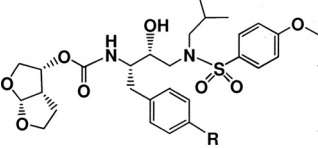
Protein structure accession numbers. The atomic coordinates of the wild-type HIV protease with TMC-126 and GS-8374 have been deposited with the RCSB Protein Data Bank and are available under accession codes 2I4U and 2I4W, respectively.
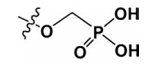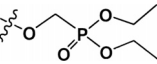
RESULTS

Phosphonate PIs and selection of GS-8374. The exploration and development of novel PIs over the past several years have led to significant improvements of their properties. In particular, the use of structure-based rational design has led to the incorporation of a bis-THF moiety at the P-2 position of the inhibitor, such as in the case of TMC-126. This inhibitor shows potent activity against both the wild-type and PI-resistant HIV-1 isolates (9, 10, 51), with the exception of viruses containing the combination of protease mutations M46I/I50V or I84V/L90M (51). Therefore, we explored various approaches to further improve the resistance profile of the TMC-126 scaffold. While a wide range of P-1′ and P-2′ substitutions did not significantly improve the properties of TMC-126 (data not shown), prior studies have demonstrated a favorable effect of certain modifications at the P-1 position (21, 22, 40). A range of compounds with substitutions at the *para* position of a P-1 phenyl moiety were investigated. Substituents, including alkyls, —OCH$_3$, —NH$_2$, —CHO, CONH$_2$, NHSO$_2$CH$_3$, and others, resulted in either the loss of activity or a deterioration of the resistance profile (data not shown). We further focused on less common substitutions, such as phosphonates, that have not previously been explored in the context of novel PIs. The addition of a phosphonic acid group at the P-1 position of TMC-126 did not lead to a significant change in the inhibition of HIV PR (K_i = 13.3 pM; Table 1), but the antiviral activity was completely eliminated, likely due to low cellular permeability. Therefore, the charged phosphonic acid was masked by various dialkyl groups, resulting in the recovery of antiviral activity (Table 1) (L. Xu et al., unpublished data). In addition, the activity of dialkylphosphonates against both mutant viruses significantly improved compared to that of the parent TMC-126. GS-8374 containing the diethylphosphonate group via a methyloxy (—OCH$_2$—) linker at the *para* position of the P-1 phenyl showed a potent antiviral effect, with the smallest shift in its activity being against the M46I/I50V and I84V/L90M mutant viruses (Table 1). Alternative options for the linker in GS-8374 were also explored by modifying the methyloxy connecting group, but this did not result in additional activity and/or a resistance profile improvement compared to that for GS-8374 (Xu et al., unpublished). Therefore, GS-8374 was selected for further characterization.

Binding of GS-8374 to HIV-1 PR. The addition of the diethylphosphonate methyloxy moiety to the P-1 of the TMC-126 scaffold reduces the K_i of the HIV-1 PR inhibition by a factor

TABLE 1. HIV-1 protease inhibition potency, antiviral activity, and resistance profile of phosphonate PIs compared to parent TMC-126

R	Compound[a]	K_i (pM)	EC$_{50}$ (nM)	Fold resistance[b]	
				M46I/I50V	I84V/L90 M
H	TMC-126	22.2 ± 9.5	0.3 ± 0.1	164	24
(phosphonic acid structure)	Phosphonic acid	13.3 ± 5.4	>50,000	ND[c]	ND
(GS-8374 structure)	GS-8374	8.1 ± 5.5	3.5 ± 1.5	2.4	0.7

[a] Data shown represent the means and standard deviations from at least two independent experiments.
[b] Fold resistance is defined as the ratio of EC$_{50}$ values for each PI-resistant mutant and a control wild-type virus.
[c] ND, not determined.

of 2- to 3-fold (Table 1). To further understand this effect, the binding kinetics of GS-8374 and TMC-126 were determined using SPR. Data were collected in a dose-response manner using a range of inhibitor concentrations. The top concentrations of both compounds were additionally tested with a longer dissociation period to enable the determination of the inhibitor on and off rates (k_{on} and k_{off}, respectively). While the association rates were similar for both GS-8374 and TMC-126, the dissociation rate of GS-8374 was too slow to be determined explicitly using this methodology (Table 2; see also Fig. S5 in the supplemental material), whereas TMC-126 had a measurable dissociation rate (Table 2). In addition to the kinetic characterization, the binding of GS-8374 and TMC-126 to HIV-1 PR were profiled thermodynamically by ITC. Data were collected using a competition experiment with acetyl-pepstatin. The binding of GS-8374 and TMC-126 to HIV-1 PR is characterized by similar free binding energies of −15.2 and −15.9 kcal/mol, respectively (Table 2). However, unlike TMC-126, which binds to PR with a favorable enthalpy but an unfavorable entropy, both the enthalpic and entropic components contribute favorably to the interaction of GS-8374 with HIV-1 PR.

Structural analysis of GS-8374 interactions with HIV-1 PR. The X-ray structures of both GS-8374 and the parent scaffold,

TABLE 2. Kinetic and thermodynamic parameters of binding of GS-8374 and TMC-126 to HIV-1 protease

Binding parameter[a]	GS-8374	TMC-126
Kinetic		
k_a (M^{-1} s^{-1})	2.08×10^6	2.76×10^6
k_d (s^{-1})	$<1.00 \times 10^{-6}$	3.81×10^{-5}
K_D (pM)[b]	<0.48	13.6
Thermodynamic		
ΔG (kcal/mol)	−15.2 ± 0.2	−15.9 ± 0.2
ΔH (kcal/mol)	−13.5 ± 0.2	−17.1 ± 0.2
$-T\Delta S$ (kcal/mol)	−1.7 ± 0.4	1.2 ± 0.4
K_D[c] (pM)	7.1 ± 1.1	2.0 ± 0.2

[a] Data shown represent the means and standard deviations from three independent experiments.
[b] K_D, equilibrium dissociation constant, calculated as a ratio of k_d/k_a.
[c] K_D, equilibrium dissociation constant.

TMC-126, were determined at 1.5-Å resolution (4). Both compounds bind HIV protease similarly, and their backbones are superimposable (Fig. 2A). Similar networks of hydrogen bonds are also observed. A buried water molecule forms four hydrogen bonds: two connecting the water hydrogens to the sulfonamide and the carbamate carbonyl oxygen atoms and two between the water oxygen and the backbone NH of Ile-50 and Ile-250. The hydroxyl group of each PI forms a hydrogen bond with the catalytic Asp-225, and both oxygen atoms of the bis-tetrahydrofuran rings are involved in hydrogen bonding with the backbone N-H of Asp-229 and Asp-230. The main conformational difference between the cocrystallized structures of TMC-126 and GS-8374 resides in the first tetrahydrofuran ring. In the new envelope conformation of the tetrahydrofuran ring present in bound GS-8374, the oxygen is flipped upwards, considerably elongating the hydrogen bond to the backbone NH of Asp-229 from 1.78 Å to 2.12 Å (Fig. 2B and C). This weaker hydrogen bond is consistent with the smaller change in enthalpy observed in ITC experiments upon binding of GS-8374 to the protease compared to the change observed for TMC-126 (Table 2).

The TMC-126 carbamate NH forms a weak hydrogen bond (2.48 Å) with the Gly-227 carbonyl oxygen (Fig. 2B). Upon GS-8374 binding, the orientation of the Gly-227 carbonyl changes, placing the oxygen 2.72 Å away from the carbamate NH in an almost perpendicular arrangement (Fig. 2C). This loss of hydrogen bonding also contributes to the minor decrease of binding enthalpy.

The electron density for GS-8374, including the di(ethyl) methoxyphosphonate group, is well-defined. The conformation of the phosphonate is constrained in a position that places one ethyl group in a hydrophobic cleft created between Phe-253, located on the flap, and Pro-81 on the opposite subunit (Fig. 2D and E). Several van der Waals contacts are observed between the phosphonate ethyl group and both the phenyl group of Phe-253 and the Pro-81 ring. The conformational entropy paid by rigidifying the flexible ethylphosphonate seems to be easily overcome by desolvation of the hydrophobic cleft on the protein surface, as evidenced by the observed favorable entropic gain upon GS-8374 binding (Table 2).
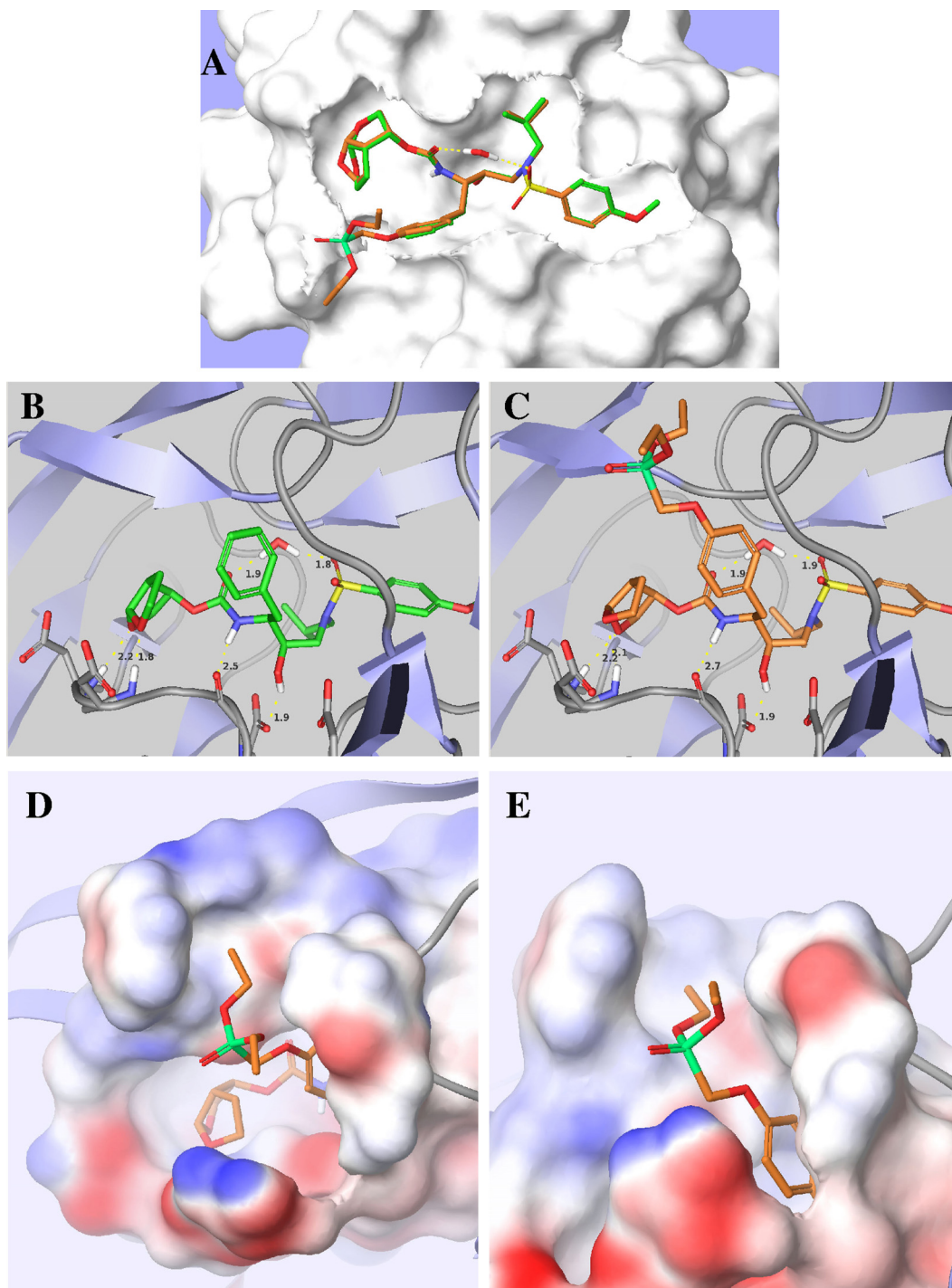
FIG. 2. Binding of GS-8374 and TMC-126 in the active site of HIV-1 protease. (A) Overlap of GS-8374 and TMC-126; (B) view of solvent-accessible surface of HIV-1 protease along with TMC-126; (C) view of solvent-accessible surface of HIV-1 protease along with the diethylphosphonate moiety of GS-8374; (D and E) top view (D) and front view (E) of diethylphosphonate group of GS-8374 bound in the active site of HIV-1 protease.

GS-8374 inhibition of HIV-1 and host proteases in comparison with other PIs. GS-8374 is a competitive tight-binding inhibitor of HIV-1 protease with a mean K_i value of 8.1 pM. Compared to clinically approved PIs, GS-8374 together with darunavir is the most potent inhibitor of HIV-1 PR (Table 3).

In addition to interacting with the target enzyme, various PIs have been reported to inhibit the activity of host proteases. Thus, GS-8374 and other PIs were tested for their potential to inhibit host aspartic proteases, including cathepsin D, renin, and β-secretase. None of the tested PIs inhibited renin or

TABLE 3. Inhibition of HIV-1 protease and human proteases in the presence of GS-8374 or clinically approved PIs

Protease inhibitor	HIV-1 protease K_i (pM)[a]	Host protease IC$_{50}$ (μM)[a]	
		Cathepsin D	Proteasome
GS-8374	8.1 ± 5.5	>30	>30
Darunavir	4.6 ± 2.8	>30	>30
Lopinavir	37.1 ± 15.7	>30	17.4 ± 1.7
Atazanavir	47.9 ± 17.8	>30	19.4 ± 3.9
Saquinavir	221 ± 23	21.1 ± 1.6	2.1 ± 1.2
Ritonavir	314 ± 39	0.39 ± 0.07	8.4 ± 1.0
Amprenavir	345 ± 72	>30	>30
Indinavir	571 ± 81	>30	>30
Nelfinavir	732 ± 113	>30	2.9 ± 1.1

[a] Data shown represent the means and standard deviations from at least two independent experiments.

TABLE 5. Cytotoxicity of GS-8374 and clinically approved PIs in various human cell lines

Protease inhibitor	CC$_{50}$ (μM)[a]			
	MT-2	MT-4	HepG2	HEK293T
GS-8374	>100	45.6 ± 15.3	61.3 ± 13.7	60.3 ± 8.7
Darunavir	>100	57.1 ± 19.0	95.5 ± 6.7	>100
Lopinavir	67.9 ± 7.5	20.3 ± 3.4	27.8 ± 4.2	34.3 ± 2.5
Atazanavir	79.8 ± 18.9	29.7 ± 6.6	26.5 ± 2.6	32.9 ± 15.8
Saquinavir	32.3 ± 13.0	7.1 ± 2.3	12.4 ± 3.2	17.4 ± 3.4
Ritonavir	65.0 ± 5.4	15.3 ± 3.5	18.4 ± 2.5	14.3 ± 0.8
Amprenavir	>100	47.5 ± 12.7	98.4 ± 6.5	>100
Indinavir	>100	55.1 ± 10.2	74.7 ± 14.6	>100
Nelfinavir	19.1 ± 6.8	4.9 ± 1.2	7.4 ± 0.8	10.3 ± 0.1

[a] Data shown represent the means and standard deviations from at least two independent experiments.

β-secretase at concentrations as high as 30 μM (data not shown). However, the inhibition of cathepsin D activity was detected for some of the original PIs, such as ritonavir and saquinavir, whereas no inhibition was observed with the other PIs, including GS-8374 (Table 3). It has also been shown that treatment with certain PIs reduces the proteasome-mediated degradation of specific cellular proteins (30); therefore, we assessed the potential of GS-8374 to inhibit the chymotrypsin-like proteasome activity. Similar to darunavir, amprenavir, and indinavir, GS-8374 did not show any inhibition of proteasome activity at up to a 30 μM concentration (Table 3). In contrast, nelfinavir, ritonavir, saquinavir, atazanavir, and lopinavir exhibited some level of inhibitory activity in the proteasome assay, with IC$_{50}$s ranging from 2.1 to 19.4 μM. Together, these results indicate a high degree of selectivity of GS-8374 toward HIV-1 protease relative to that of host proteases.

Antiretroviral activity and cytotoxicity. GS-8374 was evaluated in several *in vitro* HIV-1 replication systems in both T-cell lines and primary T cells. In a 5-day assay in MT-2 and MT-4 cells, GS-8374 inhibited the HIV-1-mediated cytopathic effect with EC$_{50}$s of 3.4 and 11.5 nM, respectively (Table 4). The minor difference in potency observed between MT-2 and MT-4 cells is possibly due to the different MOIs used in the two assays and/or different levels of cellular efflux transporters in the two cell lines. Similar differences were seen for most of the

TABLE 4. Anti-HIV-1 activities of GS-8374 and clinically approved PIs in T-cell lines and primary CD4$^+$ T cells

Protease inhibitor	EC$_{50}$ (nM)[a]		
	MT-2 cells	MT-4 cells	CD4$^+$ T cells
GS-8374	3.4 ± 0.8	11.5 ± 6.7	5.0 ± 3.0
Darunavir	2.3 ± 0.8	3.7 ± 1.2	ND[b]
Lopinavir	5.6 ± 2.3	61.2 ± 16.2	10.8 ± 8.8
Atazanavir	2.2 ± 1.2	8.0 ± 3.1	0.9 ± 1.0
Saquinavir	13.6 ± 4.9	14.6 ± 4.9	22.4 ± 16.4
Ritonavir	32.2 ± 16.1	107.1 ± 24.9	13.2 ± 1.4
Amprenavir	24.0 ± 0.0	74.0 ± 23.3	ND
Indinavir	12.4 ± 4.9	42.0 ± 12.2	113.0 ± 5.2
Nelfinavir	13.2 ± 4.7	39.4 ± 7.6	37.6 ± 34.3

[a] Data shown represent the means and standard deviations from at least two independent experiments.
[b] ND, not determined.

control PIs tested in parallel. GS-8374 also exhibited potent activity in a single-cycle antiviral assay in primary CD4$^+$ T cells with an EC$_{50}$ of 5 nM. Overall, the *in vitro* activity of GS-8374 against HIV-1 was either comparable to or better than that of the clinically approved PIs. In addition, GS-8374 was active against HIV-1 in primary macrophages with an EC$_{50}$ of 25.5 nM (Roger Ptak, Southern Research Institute, personal communication).

In subsequent studies, the testing of GS-8374 in PBMCs was extended to HIV-1 isolates representing multiple clades. GS-8374 displayed potent antiviral activity against all tested clades of HIV-1, with EC$_{50}$s ranging from 0.97 to 5.08 nM (mean EC$_{50}$ = 2.6 nM) and EC$_{90}$ values ranging from 2.99 to 9.15 nM (mean EC$_{90}$ = 6.8 nM) (see Table S9 in the supplemental material). GS-8374 was also found to be active against HIV-2, exhibiting EC$_{50}$ and EC$_{90}$ values of 3.45 and 8.25 nM, respectively.

The *in vitro* cytotoxicity of GS-8374 and other PIs was evaluated in various human cell types, including T cells (MT-2 and MT-4), liver-derived cells (HepG2), and kidney-derived cells (HEK293T) (Table 5). In all tested cell lines, GS-8374 showed a low level of cytotoxicity, with CC$_{50}$ values ranging from 45 to >100 μM. This compares favorably with the cytotoxicities of other PIs, including atazanavir and darunavir. In both MT-2 and MT-4 cells, GS-8374 achieved a selectivity index (CC$_{50}$/EC$_{50}$ ratio) of >4,000, which was again comparable to or superior to the indexes for the approved PIs.

Effect of serum proteins on activity of GS-8374. Most PIs bind extensively to serum proteins, which decreases the levels of free extracellular compound available to inhibit the virus. The *in vitro* antiviral activity of PIs corrected for serum protein binding is frequently used for the calculation of inhibitory quotients and estimation of the *in vivo* effective dose (24). The effect of HS on the activity of GS-8374 was evaluated in MT-2 cells in the presence of various concentrations of HS ranging from 10 to 50%, and the inhibitory potency was extrapolated to that for 100% HS. The extrapolated EC$_{50}$ of GS-8374 in 100% HS was 19.4 nM, representing a 3.7-fold reduction in the antiviral potency due to serum protein binding (Table 6). This effect compares favorably with the effects of atazanavir and lopinavir, which represent low- and medium-level serum binding PIs, respectively. The antiviral activity of GS-8374 was also determined in the presence of physiological concentrations of HSA and AGP. AGP affected the potency of GS-8374 substan-

TABLE 6. Effects of serum proteins on the antiviral activity of GS-8374 and control PIs

Protease inhibitor	EC_{50} (nM)[a]				
	Control	HS (50%)	HS,[b] extrapolated (100%)	HSA (40 mg/ml)	AGP (1 mg/ml)
GS-8374	5.2 ± 2.5	14.1 ± 4.1 (2.7)	19.4 (3.7)	13.2 ± 6.2 (2.5)	83.4 ± 20.2 (16.1)
Atazanavir	3.0 ± 1.4	7.1 ± 2.1 (2.4)	7.9 (2.6)	10.8 ± 0.7 (3.6)	14.5 ± 2.1 (4.8)
Lopinavir	4.1 ± 2.0	14.2 ± 1.4 (3.5)	23.2 (5.7)	12.2 ± 4.3 (3.0)	62.7 ± 54.8 (15.5)
Nelfinavir	7.7 ± 2.4	147.9 ± 60.3 (19.2)	254.8 (33.1)	40.7 ± 17.7 (5.3)	279.5 ± 152.2 (36.1)

[a] Data shown represent the means and standard deviations from at least two independent experiments in the absence (control) and presence of 50% HS, HSA, or AGP. Values in parentheses are fold change.
[b] EC_{50}s were extrapolated to 100% HS from the EC_{50}s determined in the presence of 0, 10, 20, 35, and 50% HS (from the means of three independent experiments at each HS concentration).

tially more than HSA (Table 6), indicating that AGP represents the main component sequestering GS-8374 in human serum. The more significant reduction of the activity of GS-8374 by purified AGP compared to that by complete human serum might be due to different binding properties, in part because of the presence of endogenous AGP ligands in serum that may reduce its binding capacity compared to that of the purified form of AGP. Overall, serum proteins show a moderate effect on the activity of GS-8374.

Combination studies with GS-8374. The *in vitro* antiretroviral activity of GS-8374 was tested in various combinations with representative drugs from major antiretroviral classes, including nucleoside reverse transcriptase inhibitors (NRTIs; zidovudine, tenofovir, and emtricitabine), nonnucleoside reverse transcriptase inhibitors (NNRTIs; TMC-125 and TMC-278), an integrase inhibitor (INI; elvitegravir), and PIs (atazanavir and darunavir). Combinations of tenofovir-efavirenz, stavudine-ribavirin, and GS-8374 with itself were used as controls for synergy, antagonism, and additivity, respectively. When GS-8374 was combined with any of the tested NRTIs or NNRTIs, it exhibited highly synergistic effects, with synergy score values ranging from 119 to 179 (Table 7). The combination of GS-8374 with elvitegravir produced intermediate synergy, which is in agreement with the findings of previous combination studies performed with elvitegravir showing that the lowest level of synergy among the classes tested was observed with PIs (16). Surprisingly, the combination of GS-8374 with atazanavir was highly synergistic, reaching a synergy score of

172, while the combination with darunavir was additive (Table 7). Structural similarity between GS-8374 and darunavir may explain their additive effect when they are combined. In contrast, synergy of atazanavir in combination with other PIs has been previously reported (37), possibly as an effect of increased intracellular levels of PIs due to the efflux inhibition (18, 41). Importantly, none of the tested drug combinations containing GS-8374 exhibited any antagonistic antiviral effects.

Activity of GS-8374 against PI-resistant HIV-1 strains. The initial profiling of GS-8374 against the M46I/I50L and I84V/L90M mutant viruses was suggestive of improvement in the compound resistance profile compared to that for the parent compound, TMC-126 (Table 1). To expand on this initial observation, the activity of the compound against a panel of 24 patient-derived mutant viruses with high-level phenotypic resistance to multiple clinically approved PIs was characterized using a PhenoSense assay (32). The selected viruses contained an average of 10 resistance mutations in their proteases, with each known primary PI resistance mutation being present in multiple viruses (see Table S10 in the supplemental material). GS-8374 showed a mean EC_{50} of 7.0 nM (range, 0.7 to 32 nM) against the panel of tested viruses and a mean EC_{50} fold change of 6.2 (range, 0.7- to 26-fold) relative to the values for wild-type control virus (Table 8). In contrast, darunavir showed a mean EC_{50} fold change of 30 (range, 1.0- to 158-fold). The shift in the tipranavir EC_{50} against the tested viruses was similar to that of GS-8374 (mean, 5.9-fold; range, 0.3- to 28-fold), but its absolute potency was 50- to 100-fold lower. Only 3 out

TABLE 7. Antiviral activity of GS-8374 in combination with other antiretrovirals

Drug combination[a]	Class	Net effect	Synergy score[b]	Antagonism score[b]
GS-8374 + AZT	NRTI	Highly synergistic	120 ± 19	-19 ± 22
GS-8374 + TFV	NRTI	Highly synergistic	124 ± 40	-5.8 ± 9.4
GS-8374 + FTC	NRTI	Highly synergistic	179 ± 18	-0.4 ± 0.7
GS-8374 + TMC-278	NNRTI	Highly synergistic	119 ± 42	-15 ± 10
GS-8374 + TMC-125	NNRTI	Highly synergistic	156 ± 43	-3.6 ± 7.1
GS-8374 + EVG	INI	Moderately synergistic	96 ± 40	-9.7 ± 7.1
GS-8374 + DRV	PI	Additive	25 ± 22	-16 ± 13
GS-8374 + ATV	PI	Highly synergistic	172 ± 66	-14 ± 22
Controls				
GS-8374 + GS-8374	Control	Additive	23 ± 15	-6.5 ± 6.5
d4T + RBV	Control	Highly antagonistic	5.5 ± 4.1	-404 ± 102
TFV + EFV	Control	Highly synergistic	107 ± 36	-4.3 ± 7.5

[a] AZT, zidovudine; TFV, tenofovir; FTC, emtricitabine; TMC-278, rilpivirine; TMC-125, etravirine; EVG, elvitegravir; DRV, darunavir; ATV, atazanavir; RBV, ribavirin; d4T, stavudine; EFV, efavirenz.
[b] Data shown represent the means and standard deviations from three independent experiments performed in triplicate.

TABLE 8. Compiled resistance profile data for GS-8374 and
clinically approved PIs against PI-resistant HIV-1 variants

Protease inhibitor[a]	EC_{50} (nM)		Fold change relative to WT virus[b]		No. of viruses with fold change >10 (n/24)
	Mean	Range	Mean	Range	
GS-8374	7.0	0.7–32	6.2	0.7–26	3
Darunavir	20.0	0.9–100	30	1.0–158	16
Tipranavir	624	34–3,000	5.9	0.3–28	4
Saquinavir	252	6.2–500	63	1.6–127	19
Ritonavir	232	128–3,000	207	11–268	24
Nelfinavir	624	6.5–1,500	120	1.2–342	22
Lopinavir	446	7.3–1,000	137	2.2–303	19
Indinavir	514	16–1,500	81	2.6–238	18
Amprenavir	676	21–2,000	73	2.4–221	20
Atazanavir	157	4.3–500	148	4.1–479	21

[a] Individual results for 24 analyzed multi-PI-resistant viruses determined using Monogram PhenoSense assay are presented in Fig. 3. Protease genotypes of the PI-resistant viruses and individual data are shown in Tables S10 to S12 in the supplemental material).

[b] Fold change is defined as the ratio of EC_{50}s for each PI-resistant mutant and a control wild-type virus.

of the 24 tested viruses showed >10-fold resistance to GS-8374, whereas 16/24 viruses showed >10-fold resistance to darunavir; all the other tested PIs with the exception of tipranavir exhibited >10-fold loss of activity against at least 18 out of 24 tested viruses. A graphical summary of the resistance profile of GS-8374 relative to the profiles for the other PIs with the 24 mutant viruses is shown in Fig. 3, and the corresponding numerical values are listed in Tables S11 and S12 in the supplemental material. From this limited number of isolates, it was not possible to clearly identify a specific pattern of mutations associated with the reduced susceptibility to GS-8374. The four viruses with the highest degree of resistance to GS-8374 contained a combination of mutations at positions 10, 46, 48, 54, 71, 82, and 90. However, there were viruses in the panel with the same combination of mutations but minimal resistance to GS-8374, indicating that additional secondary mutations and/or a specific polymorphism in the protease or Gag polyprotein substrate may be needed for a more significant reduction in the activity of GS-8374.

***In vitro* hepatic metabolism of GS-8374.** The structure and lipophilic nature of many PIs render them efficient substrates for metabolism by human CYP3A enzymes, and this results in impaired oral bioavailability and short half-lives. Changes de-
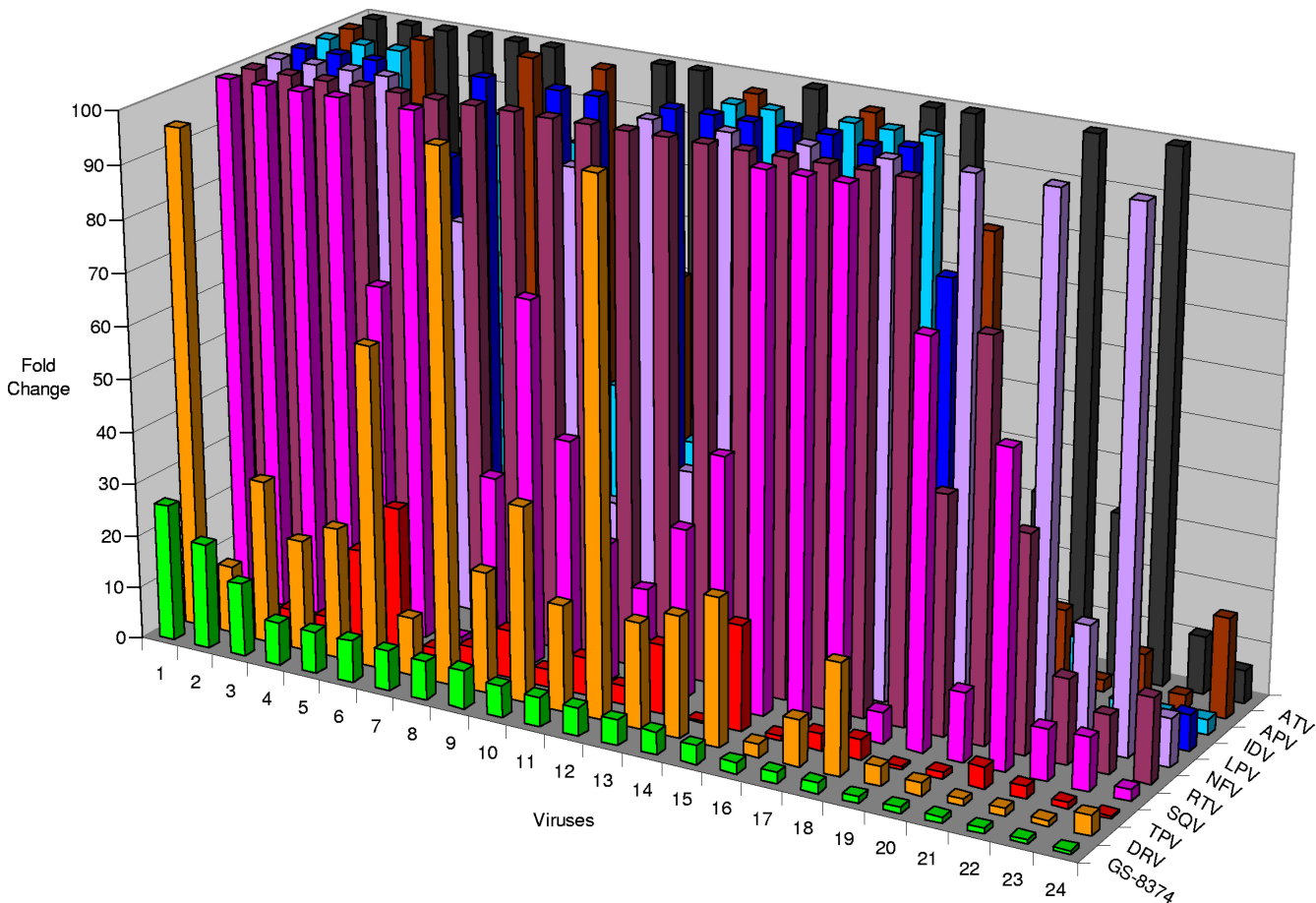

FIG. 3. Resistance profile of GS-8374. Twenty-four patient-derived multi-PI-resistant viruses were evaluated for their sensitivity to GS-8374 and clinically approved PIs using the Monogram PhenoSense assay. Genotypes of PI-resistant viruses, values for individual EC_{50}s, and fold resistance for each tested PI are presented in Tables S10, S11, and S12 in the supplemental material. ATV, atazanavir; APV, amprenavir; IDV, indinavir; LPV, lopinavir; NFV, nelfinavir; RTV, ritonavir; SQV, saquinavir; TPV, tipranavir; DRV, darunavir.
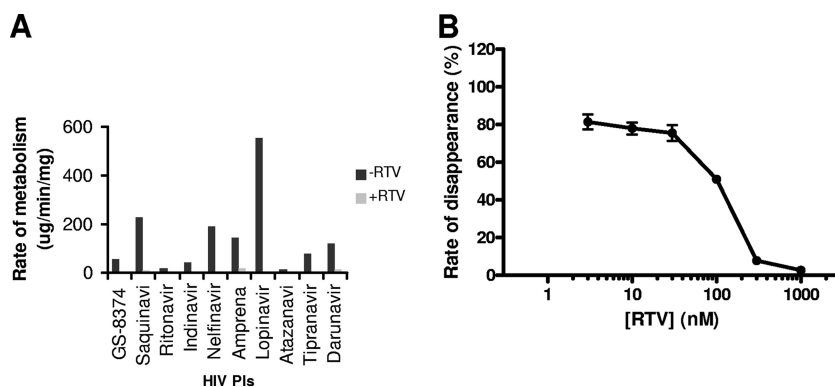
FIG. 4. Effect of ritonavir on *in vitro* hepatic metabolism of GS-8374 and clinically approved PIs. (A) PIs (3 μM) were incubated with pooled human hepatic microsomal fraction in the absence or presence of 1 μM RTV as described in Materials and Methods; (B) inhibition of GS-8374 microsomal metabolism by various concentrations of ritonavir. Data shown represent the means and standard deviations from two independent experiments performed in duplicate.

signed to improve the potency and resistance profile of PIs are often incompatible with favorable pharmacokinetic properties. Consequently, potent PIs frequently require pharmacoenhancement (boosting) to achieve sufficient systemic exposure in humans (49). The boosting is currently achieved by codosing the PIs with a subtherapeutic dose of ritonavir, a CYP3A inhibitor. In a metabolic stability assay using pooled human hepatic fraction, the approved PIs showed a wide range of metabolic rates (13 to 555 μl/min/mg). GS-8374 exhibited an intermediate rate of *in vitro* metabolism compared to the rates exhibited by these PIs (Fig. 4A). The hepatic metabolism of all tested compounds, including GS-8374, was sensitive to inhibition by ritonavir. Following a 15-min preincubation with various concentrations of ritonavir, the metabolism of GS-8374 was inhibited in a dose-dependent manner, with 50% inhibition being observed at approximately 100 nM ritonavir (Fig. 4B). The clearance of GS-8374 was blocked by >97% in the presence of 1 μM ritonavir, indicating that CYP3A enzymes are primarily responsible for its hepatic metabolism and that coadministration with the boosting dose of ritonavir would result in effective inhibition of the hepatic metabolic clearance of GS-8374.

DISCUSSION

The field of HIV protease inhibitors has evolved rapidly since the approval of saquinavir in 1995. The number of approved drugs in the PI class is higher than that for any other class of antiretrovirals. While the original PIs suffered from serious limitations, such as extreme pill burden, adverse effects, and a low barrier for resistance development, the more recently approved PIs are much improved drugs contributing to the expanded treatment options for multiple patient populations. However, only three out of the nine approved PIs are in fact being widely prescribed as part of current treatment regimens. These comprise lopinavir, atazanavir, and darunavir, all of which are used in combination with low-dose ritonavir to boost their systemic exposure. Darunavir appears to be the most versatile PI, since it has been approved for once-daily dosing in treatment-naïve patients (23) and its more favorable resistance profile allows it to be used effectively twice daily in

treatment-experienced patients (19). Although darunavir maintains its activity against a wider range of PI-resistant viruses than the other PIs available clinically (6), there still remains a relatively significant proportion of patients with PI resistance mutations who do not fully benefit from darunavir treatment (5).

A comparison of the resistance profile of darunavir with that of amprenavir demonstrated that the bis-THF moiety in the P-2 position is one of the main determinants of the improved resistance profile of darunavir (42). To further explore the possibility of improving the characteristics of PIs containing bis-THF, we have modified TMC-126, a close analog of darunavir, by introducing various substitutions at the *para* position of its P-1 phenyl residue. Among the various modifications tested, only dialkylphosphonates yielded a desirable antiviral profile, with GS-8374 being identified as the best candidate that exhibits potent and selective antiviral activity, low *in vitro* cytotoxicity, moderate serum protein binding, and synergistic activity in combination with other antiretrovirals. While GS-8374 binds to HIV-1 PR with an affinity similar to that of TMC-126, its binding shows a significant favorable contribution of the entropic component, which has not been detected in the case of TMC-126. In addition, the kinetic characterization of binding revealed a slower dissociation rate of GS-8374 that may be driven by additional interactions between the di(ethyl)phosphonate moiety and surface regions of PR distant from its active site.

Perhaps most significantly, however, characterization of the GS-8374 resistance profile against 24 patient-derived HIV-1 strains with high-level resistance to multiple PIs demonstrated that the characteristics of GS-8374 were superior to those of all the clinically approved PIs, including darunavir. GS-8374 showed the lowest mean EC$_{50}$ among all the tested PIs, and the high-level resistance (i.e., >10-fold compared to the activity against the wild type) was detected with only 3 viruses in the tested panel but 16 or more viruses with most of the other PIs. Comparison of protease sequences among the profiled viruses revealed that the level of resistance to GS-8374 is not associated with either the number of mutations or their specific pattern, suggesting that additional genotypic determinants might also affect the susceptibility to GS-8374. In fact, *in vitro*

resistance selection performed with HIV-1 passaged in the presence of increasing concentrations of GS-8374 for approximately 1 year yielded a virus isolate with approximately 15-fold resistance to GS-8374. The virus contained multiple mutations in Gag, mainly located outside cleavage sites, and the only one genotypic change in PR was a naturally occurring polymorphism, R41K (2). Further analysis demonstrated that the Gag mutations confer resistance to GS-8374, indicating a significant difficulty for the virus to select for resistance mutations in PR. Notably, noncleavage site resistance mutations in Gag were also observed in resistance selections with other novel PIs (26, 31). Some of these mutations conferred reduced replication capacity and hypersensitivity to several approved PIs.

Together, our data indicate that the addition of the diethylphosphonate methyloxy moiety leads to a marked improvement of inhibitor activity against a wide range of HIV-1 variants with high-level resistance to approved PIs. The mechanism is not fully understood for all the mutants, but it might be at least in part related to the exposure of the hydrophilic phosphonate to the solvent environment. This appears to afford more flexibility of the inhibitor when it binds to the active site of mutant forms of PR (4). Thermodynamic analysis of binding to mutant PRs demonstrated a favorable entropic compensation for the loss of enthalpy due to mutations in the inhibitor binding site. GS-8374 showed more significant entropic compensation than TMC-126 (4). It should also be noted that the linker connecting the phosphonate moiety to the P-1 phenyl residue affects both the activity and resistance profile of the inhibitors (Xu et al., unpublished), suggesting that a proper orientation and positioning of the di(alkyl)phosphonate group on the PR surface may also play some role in the mechanism. Indeed, the close examination of the crystallographic structure of GS-8374 bound to PR showed potential binding of one of the phosphonate ethyl moieties in a hydrophobic cleft on the surface of protease. It should be kept in mind that compounds with various P-1 phenyl substitutions have been previously described. One such example is brecanavir (GW-0385), a highly potent PI with a resistance profile superior to that of darunavir that has reached phase 2 clinical evaluation (11). Brecanavir contains a methylthiazole substitution of the P-1 phenyl residue, and although both the *para* position and the methoxy linker are same as in GS-8374, the resistance profile of brecanavir is less favorable (see Fig. S6 in the supplemental material).

As a class, PIs are associated with clinical off-target effects on lipid and glucose metabolism, manifested by elevated levels of cholesterol and triglycerides, type II diabetes, and a potentially increased risk for cardiovascular complications (30, 38). In an independent study published in parallel with this report, Hruz et al. (12) used both *in vitro* and *in vivo* models to assess the effects of GS-8374 on the glucose and lipid metabolism relative to those of selected clinically approved PIs. The results demonstrated a profile similar to that of atazanavir and darunavir, suggesting that GS-8374 may potentially exhibit a reduced potential for metabolism-related complications relative to that for the original PIs.

According to current HIV treatment guidelines, PIs should be coadministered with a low dose of ritonavir to increase their systemic exposure by blocking their cytochrome P450-medi-

ated metabolic clearance. *In vitro* metabolic stability studies showed that ritonavir at concentrations relevant for the clinical pharmacokinetic boosting almost completely blocks the metabolic clearance of GS-8374. Since ritonavir is a mechanism-based inhibitor of human CYP3A enzymes, the duration of its action is predicted to be sufficient to cover a 24-hour dosing interval for GS-8374 and ritonavir, provided that there is no significant alternate elimination pathway in humans that cannot be inhibited (e.g., active hepatic efflux).

In conclusion, results of the extensive pharmacological profiling of the novel phosphonate-containing HIV protease inhibitor GS-8374 support its further exploration as a potential antiretroviral agent for the treatment of a wide range of HIV-infected patients, including those with existing drug resistance.

REFERENCES

1. **Bartlett, J. A., R. DeMasi, J. Quinn, C. Moxham, and F. Rousseau.** 2001. Overview of the effectiveness of triple combination therapy in antiretroviral-naive HIV-1 infected adults. AIDS **15:**1369–1377.
2. **Callebaut, C., et al.** 2007. In vitro HIV-1 resistance selection to GS-8374, a novel phosphonate protease inhibitor: comparison with lopinavir, atazanavir, and darunavir, abstr. 16. Abstr. 16th Int. HIV Drug Resistance Workshop.
3. **Carr, A.** 2003. Toxicity of antiretroviral therapy and implications for drug development. Nat. Rev. Drug Discov. **2:**624–634.
4. **Cihlar, T., et al.** 2006. Suppression of HIV-1 protease inhibitor resistance by phosphonate-mediated solvent anchoring. J. Mol. Biol. **363:**635–647.
5. **Clotet, B., et al.** 2007. Efficacy and safety of darunavir-ritonavir at week 48 in treatment-experienced patients with HIV-1 infection in POWER 1 and 2: a pooled subgroup analysis of data from two randomised trials. Lancet **369:** 1169–1178.
6. **De Meyer, S., et al.** 2005. TMC114, a novel human immunodeficiency virus type 1 protease inhibitor active against protease inhibitor-resistant viruses, including a broad range of clinical isolates. Antimicrob. Agents Chemother. **49:**2314–2321.
7. **Detels, R., et al.** 1998. Effectiveness of potent antiretroviral therapy on time to AIDS and death in men with known HIV infection duration. Multicenter AIDS Cohort Study Investigators. JAMA **280:**1497–1503.
8. **DHHS, Office of AIDS Research Advisory Council.** 2009. Guidelines for the use of antiretroviral agents in HIV-1-infected adults and adolescents. DHHS, Office of AIDS Research Advisory Council, Washington, DC.
9. **Ghosh, A. K., B. D. Chapsal, I. T. Weber, and H. Mitsuya.** 2008. Design of HIV protease inhibitors targeting protein backbone: an effective strategy for combating drug resistance. Acc. Chem. Res. **41:**78–86.
10. **Ghosh, A. K., E. Pretzer, H. Cho, K. A. Hussain, and N. Duzgunes.** 2002. Antiviral activity of UIC-PI, a novel inhibitor of the human immunodeficiency virus type 1 protease. Antiviral Res. **54:**29–36.
11. **Hazen, R., et al.** 2007. In vitro antiviral activity of the novel, tyrosyl-based human immunodeficiency virus (HIV) type 1 protease inhibitor brecanavir (GW640385) in combination with other antiretrovirals and against a panel of protease inhibitor-resistant HIV. Antimicrob. Agents Chemother. **51:**3147–3154.
12. **Hruz, P., et al.** 2011. GS-8374, a novel HIV protease inhibitor, does not alter glucose homeostasis in cultured adipocytes or in a healthy-rodent model system. Antimicrob. Agents Chemother. **55:**1377–1382.
13. **Imaz, A., et al.** 2009. Raltegravir, etravirine, and ritonavir-boosted darunavir: a safe and successful rescue regimen for multidrug-resistant HIV-1 infection. J. Acquir. Immune Defic. Syndr. **52:**382–386.
14. **Johnson, V. A., et al.** 2009. Update of the drug resistance mutations in HIV-1: December 2009. Top. HIV Med. **17:**138–145.
15. **Kirk, J. B., and M. B. Goetz.** 2009. Human immunodeficiency virus in an aging population, a complication of success. J. Am. Geriatr. Soc. **57:**2129–2138.
16. **Ledford, R., N. Margot, M. Miller, and D. McColl.** 2007. Elvitegravir (GS-9137/JTK-303), an HIV-1 integrase inhibitor, has additive to synergistic interactions with antiretroviral drugs in vitro, abstr. 052. Abstr. 4th Int. AIDS Soc. Conf. HIV Pathogenesis, Treatment, Prevention.

17. **Little, S. J., et al.** 2002. Antiretroviral-drug resistance among patients recently infected with HIV. N. Engl. J. Med. **347:**385–394.
18. **Lucia, M. B., et al.** 2005. Atazanavir inhibits P-glycoprotein and multidrug resistance-associated protein efflux activity. J. Acquir. Immune Defic. Syndr. **39:**635–637.
19. **Madruga, J. V., et al.** 2007. Efficacy and safety of darunavir-ritonavir compared with that of lopinavir-ritonavir at 48 weeks in treatment-experienced, HIV-infected patients in TITAN: a randomised controlled phase III trial. Lancet **370:**49–58.
20. **Markgren, P. O., et al.** 2001. Determination of interaction kinetic constants for HIV-1 protease inhibitors using optical biosensor technology. Anal. Biochem. **291:**207–218.
21. **Miller, J. F., et al.** 2006. Ultra-potent P1 modified arylsulfonamide HIV protease inhibitors: the discovery of GW0385. Bioorg. Med. Chem. Lett. **16:**1788–1794.
22. **Miller, J. F., et al.** 2005. Novel P1 chain-extended HIV protease inhibitors possessing potent anti-HIV activity and remarkable inverse antiviral resistance profiles. Bioorg. Med. Chem. Lett. **15:**3496–3500.
23. **Mills, A. M., et al.** 2009. Once-daily darunavir/ritonavir vs. lopinavir/ritonavir in treatment-naive, HIV-1-infected patients: 96-week analysis. AIDS **23:**1679–1688.
24. **Morse, G. D., L. M. Catanzaro, and E. P. Acosta.** 2006. Clinical pharmacodynamics of HIV-1 protease inhibitors: use of inhibitory quotients to optimise pharmacotherapy. Lancet Infect. Dis. **6:**215–225.
25. **Murphy, E. L., et al.** 2001. Highly active antiretroviral therapy decreases mortality and morbidity in patients with advanced HIV disease. Ann. Intern. Med. **135:**17–26.
26. **Nijhuis, M., et al.** 2007. A novel substrate-based HIV-1 protease inhibitor drug resistance mechanism. PLoS Med. **4:**e36.
27. **Nolan, D.** 2003. Metabolic complications associated with HIV protease inhibitor therapy. Drugs **63:**2555–2574.
28. **Obach, R. S.** 1999. Prediction of human clearance of twenty-nine drugs from hepatic microsomal intrinsic clearance data: an examination of in vitro half-life approach and nonspecific binding to microsomes. Drug Metab. Dispos. **27:**1350–1359.
29. **Palella, F. J., Jr., et al.** 1998. Declining morbidity and mortality among patients with advanced human immunodeficiency virus infection. HIV Outpatient Study Investigators. N. Engl. J. Med. **338:**853–860.
30. **Parker, R. A., et al.** 2005. Endoplasmic reticulum stress links dyslipidemia to inhibition of proteasome activity and glucose transport by HIV protease inhibitors. Mol. Pharmacol. **67:**1909–1919.
31. **Parkin, N., C. Chappey, E. Lam, and C. J. Petropoulos.** 2005. Reduced susceptibility to protease inhibitors (PI) in the absence of primary PI resistance-associated mutations, abstr. H-1062. Abstr. 45th Intersci. Conf. Antimicrob. Agents Chemother. American Society for Microbiology, Washington, DC.
32. **Petropoulos, C. J., et al.** 2000. A novel phenotypic drug susceptibility assay for human immunodeficiency virus type 1. Antimicrob. Agents Chemother. **44:**920–928.
33. **Prichard, M., K. Aseltine, and C. Shipman, Jr.** 1993. MacSynergy II, 1.0 ed. University of Michigan, Ann Arbor, MI.
34. **Prichard, M. N., L. E. Prichard, and C. Shipman, Jr.** 1993. Strategic design

35. **Prichard, M. N., and C. Shipman, Jr.** 1990. A three-dimensional model to analyze drug-drug interactions. Antiviral Res. **14:**181–205.
36. **Richman, D. D., et al.** 2004. The prevalence of antiretroviral drug resistance in the United States. AIDS **18:**1393–1401.
37. **Robinson, B. S., et al.** 2000. BMS-232632, a highly potent human immunodeficiency virus protease inhibitor that can be used in combination with other available antiretroviral agents. Antimicrob. Agents Chemother. **44:**2093–2099.
38. **Sax, P. E., and P. Kumar.** 2004. Tolerability and safety of HIV protease inhibitors in adults. J. Acquir. Immune Defic. Syndr. **37:**1111–1124.
39. **Sigurskjold, B. W.** 2000. Exact analysis of competition ligand binding by displacement isothermal titration calorimetry. Anal. Biochem. **277:**260–266.
40. **Spaltenstein, A., W. M. Kazmierski, J. F. Miller, and V. Samano.** 2005. Discovery of next generation inhibitors of HIV protease. Curr. Top. Med. Chem. **5:**1589–1607.
41. **Storch, C. H., D. Theile, H. Lindenmaier, W. E. Haefeli, and J. Weiss.** 2007. Comparison of the inhibitory activity of anti-HIV drugs on P-glycoprotein. Biochem. Pharmacol. **73:**1573–1581.
42. **Surleraux, D. L., et al.** 2005. Discovery and selection of TMC114, a next generation HIV-1 protease inhibitor. J. Med. Chem. **48:**1813–1822.
43. **Swanstrom, R., and J. Erona.** 2000. Human immunodeficiency virus type-1 protease inhibitors: therapeutic successes and failures, suppression and resistance. Pharmacol. Ther. **86:**145–170.
44. **Tamalet, C., J. Fantini, C. Tourres, and N. Yahi.** 2003. Resistance of HIV-1 to multiple antiretroviral drugs in France: a 6-year survey (1997-2002) based on an analysis of over 7000 genotypes. AIDS **17:**2383–2388.
45. **Velazquez-Campoy, A., Y. Kiso, and E. Freire.** 2001. The binding energetics of first- and second-generation HIV-1 protease inhibitors: implications for drug design. Arch. Biochem. Biophys. **390:**169–175.
46. **Vittinghoff, E., et al.** 1999. Combination antiretroviral therapy and recent declines in AIDS incidence and mortality. J. Infect. Dis. **179:**717–720.
47. **Wensing, A. M., and C. A. Boucher.** 2003. Worldwide transmission of drug-resistant HIV. AIDS Rev. **5:**140–155.
48. **Wensing, A. M., N. M. van Maarseveen, and M. Nijhuis.** 2010. Fifteen years of HIV protease inhibitors: raising the barrier to resistance. Antiviral Res. **85:**59–74.
49. **Xu, L., and M. C. Desai.** 2009. Pharmacokinetic enhancers for HIV drugs. Curr. Opin. Invest. Drugs **10:**775–786.
50. **Yazdanpanah, Y., et al.** 2009. High rate of virologic suppression with raltegravir plus etravirine and darunavir/ritonavir among treatment-experienced patients infected with multidrug-resistant HIV: results of the ANRS 139 TRIO trial. Clin. Infect. Dis. **49:**1441–1449.
51. **Yoshimura, K., et al.** 2002. A potent human immunodeficiency virus type 1 protease inhibitor, UIC-94003 (TMC-126), and selection of a novel (A28S) mutation in the protease active site. J. Virol. **76:**1349–1358.
52. **Yusa, K., and S. Harada.** 2004. Acquisition of multi-PI (protease inhibitor) resistance in HIV-1 in vivo and in vitro. Curr. Pharm. Des. **10:**4055–4064.
53. **Zolopa, A. R.** 2010. The evolution of HIV treatment guidelines: current state-of-the-art of ART. Antiviral Res. **85:**241–244.